ARTICLE

doi:10.1038/nature13884

Life cycles, fitness decoupling and the evolution of multicellularity

Katrin Hammerschmidt[1]*, Caroline J. Rose[1]*, Benjamin Kerr[2] & Paul B. Rainey[1,3]

Cooperation is central to the emergence of multicellular life; however, the means by which the earliest collectives (groups of cells) maintained integrity in the face of destructive cheating types is unclear. One idea posits cheats as a primitive germ line in a life cycle that facilitates collective reproduction. Here we describe an experiment in which simple cooperating lineages of bacteria were propagated under a selective regime that rewarded collective-level persistence. Collectives reproduced via life cycles that either embraced, or purged, cheating types. When embraced, the life cycle alternated between phenotypic states. Selection fostered inception of a developmental switch that underpinned the emergence of collectives whose fitness, during the course of evolution, became decoupled from the fitness of constituent cells. Such development and decoupling did not occur when groups reproduced via a cheat-purging regime. Our findings capture key events in the evolution of Darwinian individuality during the transition from single cells to multicellularity.

Cooperation has a central role in the evolution of multicellularity[1–8]. Even under laboratory conditions, simple undifferentiated groups of cooperating cells readily evolve; however, such groups are often short lived: selection typically favours the evolution of cheats[9–14]. Cheats are cells that do not contribute towards group integrity, but nonetheless take advantage of the benefit that accrues from being part of a collective[7]. In the absence of cheater-suppression mechanisms, cheats may prosper to the point where the integrity of any newly emerged group is compromised[15–18]. The problem of cheating has led to the suggestion that the evolution of mechanisms for cheater suppression is a critical step in the transition to multicellularity[18–21]. In this Article we explore an alternative possibility; namely, that cheats may play a critical role in a simple multicellular life cycle where the central problem is not cheater suppression, but rather controlled generation of this phenotype[22].

The evolution of simple groups of bacteria occurs repeatedly when populations of the bacterium *Pseudomonas fluorescens* are propagated in spatially structured microcosms[9,23,24]. Such collectives—'wrinkly spreader' (WS) mats—arise by spontaneous mutations from the ancestral 'smooth' (SM) genotype[23,25]. The mutations cause WS cells to overproduce a cell–cell glue[25–27] that holds daughter cells together following cell division[28]. The net effect is a cellular mat that colonizes the air–broth interface. Although glue production is costly to individual cells, the trait spreads[29] because the group of mat-forming cells reaps an advantage (access to oxygen) that is denied to individual cells[9].

The life span of WS mats is brief: selection acting on individual cells favours mutant types that cheat. Cheating cells are phenotypically SM and no longer produce adhesive glues[9]; nonetheless they take advantage of the benefit that accrues from being part of the mat. In the absence of any mechanism of cheater repression, cheats prosper—ultimately weakening the fabric of the mat to the point where it collapses[9].

While cheats pose a significant problem, the tension between cooperating and cheating cells could fuel evolution[22,30,31]. Consider a newly emergent WS mat. In the absence of a means of collective-level reproduction, the mat, like soma, is an evolutionary dead end. The emergence of cheats however is guaranteed. While cheats may destroy the mat, they also stand as a means of mat reproduction, provided they can regenerate the mat. The cycling between WS groups and SM cells—driven by the niche-constructing activities of each type[32]—has the potential to generate a primitive life cycle[30] (Fig. 1a, left panel) and with this the possibility that WS groups might participate, even just marginally, as units of selection in the process of Darwinian evolution[33].

Embracing cheats

To test the plausibility of the idea that SM cells might function as the seeds for a new generation of WS mats, we propagated mats under a regime in which SM cells were integral to mat reproduction (Fig. 1a, left panel) (this treatment stands in stark contrast to a regime discussed below in which cheats are purged (Fig. 1a, right panel)). Each generation was founded by a single WS genotype (Fig. 1b). For lines to persist WS mats had to remain intact (viable) until the end of phase I, and be fecund (produce SM types). In addition, during the three-day phase II period, SM cells were required to transition back to WS. On completion of the cycle a single colony of the most dominant WS type was transferred to a fresh microcosm ensuring new WS mats arise through a bottleneck and are thus re-established free of within-mat conflicts[5,34].

Transitioning between group and single-cell phases relies initially upon mutation and poses significant challenges. In an initial experiment in which 120 lines were required to repeatedly transition between WS and SM states, all lines went extinct by the sixth life-cycle generation. Extinction was primarily due to insufficient SM-cell production before day six of phase I (Fig. 1c).

Given the prominent role of cheats and the requirement for mutation to transition each phase of the life cycle, the persistence of lines through six generations is surprising: it indicates a capacity for innovation. Such a capacity might, under different circumstances, provide opportunity for evolutionary refinement to the point where cycling through phases could come under developmental control.

Most non-neutral mutations are deleterious and thus prone to eventually disrupt the life cycle. Persistence is therefore likely to depend on viable lines having an opportunity to export their success to a new microcosm by division of the lineage. Were the splitting of viable lines to operate concomitantly with the elimination of unsuccessful lines then selection

[1]New Zealand Institute for Advanced Study and Allan Wilson Centre for Molecular Ecology & Evolution, Massey University, Auckland 0745, New Zealand. [2]Department of Biology and BEACON Center for the Study of Evolution in Action, University of Washington, Seattle, Washington 98195, USA. [3]Max Planck Institute for Evolutionary Biology, Plön 24306, Germany.
*These authors contributed equally to this work.

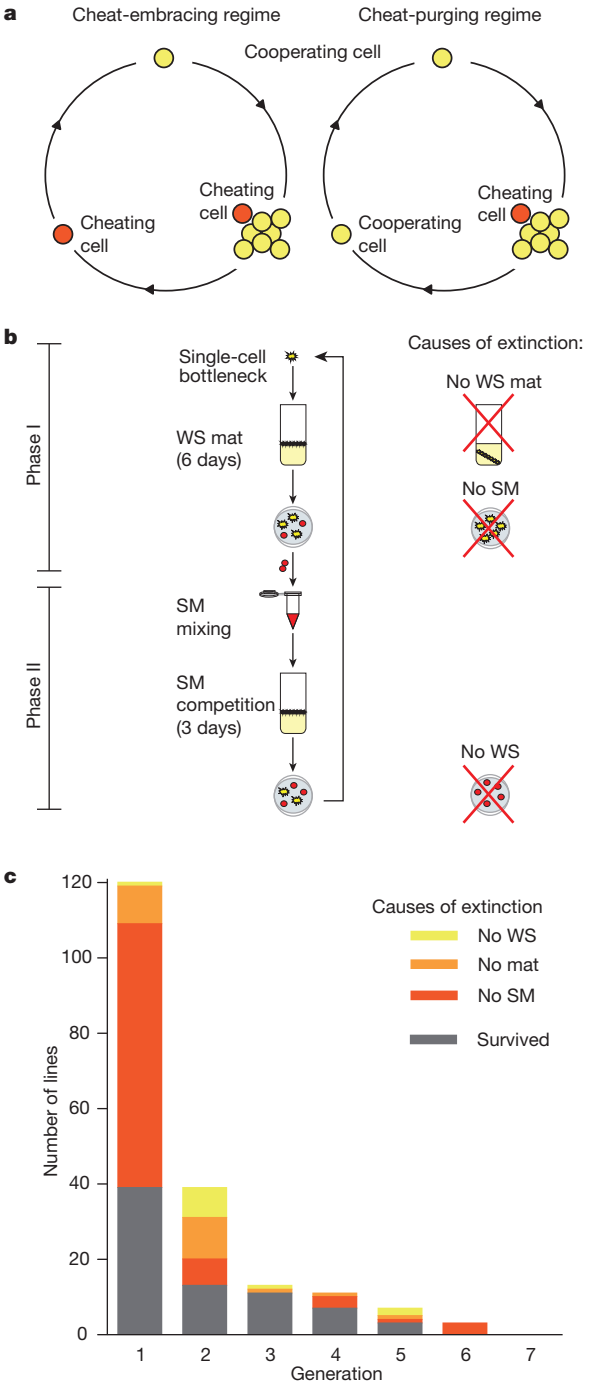

Figure 1 | Experimental regimes and extinction dynamics. **a**, Cheat-embracing (CE) and cheat-purging (CP) regimes. **b**, Each line is founded by a single WS genotype (yellow). After 6 days in phase I cells are harvested, plated and screened for SM colonies (red). Pooled SM colonies found phase II. After 3 days cells are harvested, plated and screened for WS colonies. A single WS colony of the dominant type founds the next generation. To avoid extinction, the WS mat of each line must be intact at the end of phase I and WS types must have produced SM cells; by the end of phase II, SM types must have produced WS cells. **c**, Persistence of lines ($n = 120$) and causes of extinction.

among lineages might allow the possibility for life-cycle-enhancing mutations, which are beneficial over the longer time scale of the life cycle, to outrun life-cycle-disrupting mutations[16,35,36].

Adaptive evolution and fitness decoupling

To allow for selection among lines, we took 120 microcosms, each containing a single WS mat, and divided these into 15 replicate populations,

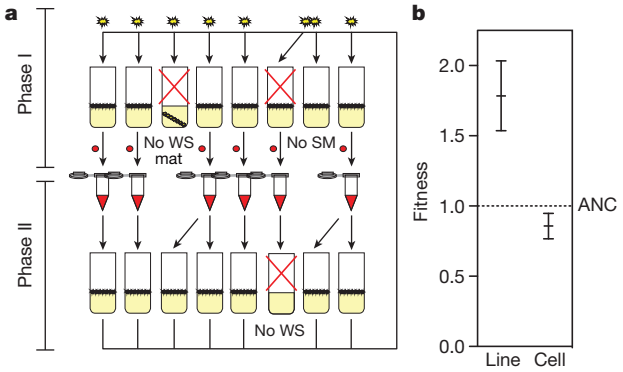

Figure 2 | Evolution under the CE regime. **a**, Lines ($n = 120$) are arranged as 15 replicate populations of 8 lines each (one replicate is depicted). The experiment involved a total of 2,400 microcosms and 140 days of selection. Extinction events provide opportunity for viable lines to reproduce. Reproduction allows export of a viable line to a new microcosm. Lines marked for reproduction were chosen at random and replacements took place within the same replicate. **b**, Fitness of derived lines and their single cell constituents relative to ancestral (ANC) types: line fitness increased significantly, whereas cell-level fitness decreased. One lineage generation was performed for each of three replicate fitness assays for each line. Error bars are s.e.m., based on $n = 14$.

each composed of 8 lines (Fig. 2a). Lines that failed to complete the life cycle provided an opportunity for viable lines to export their success to a new microcosm. Upon the demise of a particular lineage, a viable line within the same replicate was chosen at random and allowed to replace the extinct type (Fig. 2a). Extinction occurred at high frequency resulting in ~5 replacements per generation (per replicate). After ten life-cycle generations each population housed viable lines. Selection on lineage viability—and concomitantly fecundity—was thus central to persistence.

To determine the course of evolution, the fitness of isolates from evolved lines was measured relative to ancestral types. A single WS genotype representative of each population (of eight lines) was taken at the end of the selection period (see Methods and Extended Data Fig. 1a). In addition, 15 independent WS genotypes were obtained one mutational step from the ancestral SM genotype, thus providing a 'baseline' reference for ancestral fitness (see Methods and Extended Data Fig. 1a). All representative WS genotypes were competed against a *lacZ*-marked reference strain (see Methods and Extended Data Fig. 1b, left panel), allowing the competitive performance of all ancestral and evolved types to be assessed against a single common genotype[22]. From a multi-level selection perspective[37], any trait may have different impacts on the fitness of cycling lines and individual cells. To address this issue, we introduce two different fitness measures. Fitness of lines was defined as the number of WS mat offspring left relative to the marked competitor (Extended Data Fig. 1b, left panel); and cell fitness was assessed as the total number of cells contained within individual mats (irrespective of WS or SM type) at the end of the phase I period. Additional measures of cell-level performance are described below.

Fitness of evolved lines—as determined by the ability to leave mat offspring relative to ancestral types—improved significantly ($\chi^2 = 4.262$, degrees of freedom (d.f.) = 1, $P = 0.039$; Fig. 2b and Extended Data Table 1a). This is consistent with an evolutionary response to selection and shows that when SM cells are integral to the reproduction of WS mats, lines not only persist, but their ecological performance improves.

While fitness of evolved lines improved, cell fitness significantly decreased ($t_{79} = 3.092$, $P = 0.0027$; Fig. 2b and Extended Data Table 1a). This is a notable result: success at the level of evolving lineages has come at a cost to the individual cells of which the lines are composed. The fact that fitness of the evolved lines is no longer explicable in terms of the fitness of individual cells indicates that lineage fitness has become decoupled from individual cell fitness. This is consistent with theoretical predictions that during major evolutionary transitions selection shifts

from the lower (cell) to the higher (collective) level[2,38]. With such a shift arises a new kind of biological individual whose emergence is likely to curtail the independent evolution of lower-level entities[5].

Phenotypic traits underpinning lineage improvement

Traits inherent in the individual cells must explain the improved reproductive capacity of lines[37]. To explore adaptations that contributed to increased fitness of lines, life history properties were determined relative to ancestral types. Three replicate microcosms of each representative genotype were destructively sampled each day throughout phase I and II and the frequency of each type determined. With interest in the possibility that selection might have tuned life history characteristics to suit the duration of each phase, the number of days of propagation was doubled in both phase I (12 days) and phase II (6 days).

Evolved lines increased their capacity to generate the phenotype required for the next stage of the life cycle. This was evident in both phases: the new type was produced earlier and more reliably compared to the ancestral baseline lineages ($\chi^2 = 5.442$, d.f. = 1, $P = 0.0197$; Fig. 3a and Extended Data Table 1b). Moreover it was maximal at day six, suggesting tuning to the periodicity of the selection regime. Enhanced capacity to generate each stage of the life cycle was not explained by an increase in total cell density (density of the ancestral lineages was greater than that of the derived types $F_1 = 51.521$, $P < 0.0001$; Fig. 3b and Extended Data Table 1b).

The level of SM occurrence in phase I, and WS occurrence in phase II, is strongly related to line fitness (Extended Data Fig. 2a, b) in both the derived and ancestral types (evolved: $\chi^2 = 12.324$, d.f. = 1, $n = 14$, $P = 0.0004$; baseline: $\chi^2 = 22.801$, d.f. = 1, $n = 15$, $P < 0.0001$; Extended Data Table 2). Notably, five ancestral lines with high fitness had a tendency towards early production of the next life phase of the life cycle (Extended Data Fig. 2a). After selection, this propensity for reliable production was present in the majority of lines (Extended Data Fig. 2b). In successful lines—those lines capable of completing the life cycle—this was not attributable to an increase in the number of cells in the next phase of the life cycle ($F_1 = 0.589$, $P = 0.4431$; Extended Data Fig. 3a and Extended Data Table 1b), nor to a change in the proportion of cells of the next phase ($F_1 = 1.701$, $P = 0.1926$; Extended Data Fig. 3b and Extended Data Table 1b). In fact the proportion of cells (and number of cells) marking the next stage of the life cycle was often higher in ancestral lineages (Extended Data Figs 3a, b).

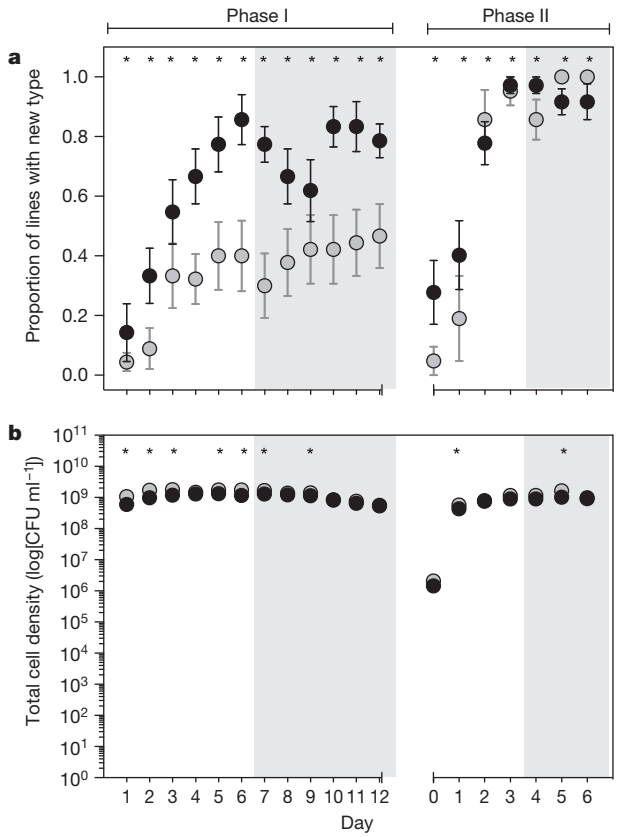

Figure 3 | Life history traits under the CE regime. **a**, Proportion of lines producing the morphotype required for the next phase of the life cycle (that is, SM from WS during phase I and WS from SM during phase II). **b**, Total cell density. Black, derived; grey, ancestral. Grey shaded panels indicate the extension of each phase as compared to the selection regime. Error bars are s.e.m., based on $n \leq 15$. *$P < 0.05$, using a generalized linear model (error structure: binomial; link function: logit) and subsequent post hoc contrasts per day for **a**; and analysis of variance (ANOVA) and subsequent post hoc contrasts per day for **b**. CFU, colony forming unit.

The increase in the frequency of occurrence of the alternative cell type suggests that the transition rate between stages of the life cycle—a form of development—may have been the focus of selection. However, an alternative possibility is that the growth rate of cells has increased such that it is more likely for a given cell type (for example, SM) to reach critical numbers before the end of the phase in which it was generated (for example, phase I). Furthermore, higher cell growth could lead to a greater cumulative number of cell divisions and thus an increased chance of generating the next cell type (for example, WS during phase II), however the abundance patterns in Fig. 3b stand in contrast to this idea. A simple mathematical model shows that the possibilities for producing cells of the opposing type via evolution of increased rates of switching readily outpaces any such possibilities arising from improvement in cell growth rate[31]. Nonetheless, to see whether growth rate had changed we determined the maximum growth rate of SM cells.

Compared to the growth rate of SM cells harvested from the ancestral lineages, the growth rate of SM cells harvested from the derived CE lines did not increase ($t_{74} = 1.527$, $P = 0.1315$; Extended Data Fig. 4 and Extended Data Table 1a). This leaves increase in the rate of transition as a clear remaining explanation for the enhanced likelihood of detecting the new type in derived lines.

Natural selection can operate on a trait at any given hierarchical level provided the trait is heritable and covaries with fitness at that level, but determining the appropriate level is challenging, especially during transitions where selection is expected to act simultaneously at multiple levels[2,39]. To discern the level of selection at which traits are associated with fitness we performed a regression and correlation analysis on traits of lines and the single cells of which they are composed. The increased capacity to transition from WS to SM predicts line fitness in the derived lineages (Extended Data Figs 5a, b and Extended Data Table 2). Moreover, line fitness is not related to, and therefore cannot be explained by, the competitive performance of single cells (Extended Data Fig. 5b). Increased line fitness is therefore a probable product of selection on properties favouring transitions between life cycle phases—a developmental programme—rather than isolated success of cells within the phases.

Genetic traits underpinning lineage improvement

The capacity for the fittest lines to transition through phases of the life cycle was markedly more rapid and reliable in derived lines compared to ancestral types (Extended Data Fig. 6). Notable was the phenotypic similarity between recurrences suggestive of a specific switch-like mechanism. The genome of the fittest lineage, line 17, was sequenced at generations 4 (WS_8) and 11 (WS_{22}) (Extended Data Fig. 7a). In addition, four independent replicate colonies of the 11-generation WS type (WS_{22}) were transferred through three additional rounds of the two-phase life cycle culminating in four independent generation-14 WS types: the genome of one of these WS types (WS_{28}) was sequenced, plus its immediate SM predecessor (SM_{27}) (Extended Data Fig. 7a).

If the life cycle is initially driven by spontaneous mutation, then seven mutations should distinguish generation-4 WS (WS_8) from ancestral SM (SM_1). Comparative analysis revealed five mutations in loci known to effect expression of WS and SM types[23]. Next we interrogated the

genome of the generation-11 WS (WS_{22}). This differed from the ancestral SM type by 53 mutations (Supplementary Table 1). This unexpectedly large number of mutations is a consequence of an elevated mutation rate attributable to a single nucleotide polymorhpism in *mutS* (A1489C, which leads to a Tyr497Pro substitution).

An obvious question is whether the *mutS* (A1489C) mutation has a direct role in promoting switching. An alternative possibility would be that *mutS* increased the probability of a different mutation that directly caused elevated switching and then hitchhiked with the switch-causing mutation. The mutant *mutS* allele was reverted to wild type and the capacity of line-17 wild-type *mutS* ($mutS^{WT}$) to pass rapidly and repeatedly through phases of the life cycle was checked. The $mutS^{WT}$ line was significantly impaired in this capacity, indicating that switching depends directly on *mutS*.

The genome of a single generation-14 WS (WS_{28}) was next compared to its immediate SM (SM_{27}) progenitor (Extended Data Fig. 7a and Supplementary Table 1). Because of the mutator background, several mutations had fixed in the WS genome; however, of note was a frameshift mutation in a tract of seven guanine residues in *wspR* (nucleotides 742–748) resulting in an additional guanine in the SM type. *wspR* encodes a diguanylate cyclase and is one of 39 such genes that can, in principle, underpin expression of the WS phenotype (and its loss)[23,26,27]. Given that the tract of guanine residues overlaps the active site of WspR (ref. 40) we considered the possibility that the *mutS* mutation might have turned *wspR* into a genetic switch enabling rapid and predictable transitioning between SM and WS through expansion and contraction of the tract of guanines[41] in a manner reminiscent of a contingency locus[42]. A disproportionate increase in the number of frameshift mutations in the *mutS* genotype, specifically in tracts of guanine (and corresponding cytosine) residues (Supplementary Table 1), supports this possibility[43].

The DNA sequence of *wspR* was obtained from every WS and SM genotype that arose from fourfold replication of the generation-11 line-17 WS through three additional 'expedited' rounds of the life cycle (Extended Data Fig. 7a). As shown in Extended Data Fig. 7b many of the transitions between WS and SM from generation 10 onward correlated with expansion (*wspR* OFF) or contraction (*wspR* ON) of the guanine tract. In a control experiment, performed with line-17 $mutS^{WT}$, the slower and less reliable transition between phenotypic states did not, with a single exception, involve the tract of guanine residues.

The existence of a genetic switch in line-17 is highly advantageous to the collective: it strengthens heritability between recurrences; integrates both phases into essentially a single entity; and constitutes a critical first step in the emergence of differentiation[4]. Genome sequencing showed that the *mutS*-dependent switch arose in just a single lineage, but fixed in all eight populations of the replicate. Its evolution was reliant on earlier mutations in Wsp that preserved functionality of the pathway while ensuring constitutive activation of WspR[25]. It also depended on mutations elsewhere in the genome that exhausted alternate genetic routes to WS. Together, this set of prior mutations, in conjunction with *mutS* (A1489C), conferred special significance to the tract of guanine residues in *wspR*. While dependency on *mutS* might seem a dangerous liaison, the life cycle provides ample opportunity for purifying selection to maintain integrity of the SM type and refine the switch.

Purging cheats

Reproduction of mats in the cheat-embracing (CE) regime underpinned significant evolutionary change. The causative factor is of central interest. While it is possible that a life cycle of two phases is key, reproduction via a bottleneck phase, combined with selection among lineages, may be sufficient. To test for such a possibility we performed a control experiment in which WS mats were propagated under a 'cheat-purging' (CP) regime. The sole difference between the CP and CE regimes is the cell phenotype that passes through the bottleneck: under the CP regime the cell passing through the bottleneck is a WS cell (Fig. 1a, right panel). Reproduction via the CP regime is analogous to fragmentation.

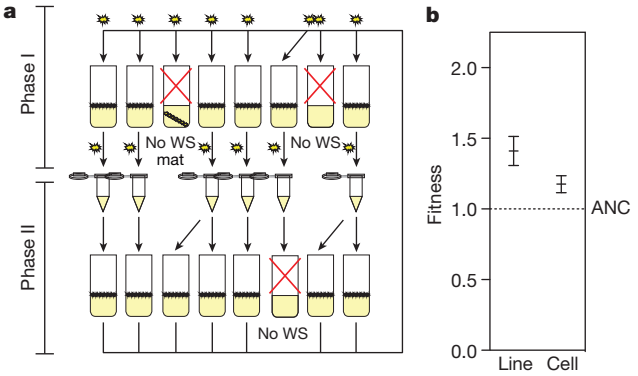

Figure 4 | Evolution under the CP regime. **a**, Lines ($n = 120$) are arranged as 15 replicates of eight (one replicate is depicted). The experiment involved a total of 2,400 microcosms. Extinction events provide an opportunity for viable lines to reproduce. Reproduction allows export of a viable line to a new microcosm. Lines marked for reproduction were chosen at random and replacements took place within the same replicate. **b**, Fitness of derived lines and their single cell constituents relative to ancestral (ANC) types: both line and cell-level fitness increased significantly. One lineage generation was performed for each of three replicate fitness assays for each line. Error bars are s.e.m., based on $n = 15$.

Conventional wisdom predicts that the CP regime will have the greatest evolutionary potential. Indeed, after 10 generations of lineage selection (Fig. 4a) fitness of evolved lines improved significantly ($\chi^2 = 15.737$, d.f. $= 1$, $P < 0.0001$; Fig. 4b and Extended Data Table 1a). However, this was accompanied by a similar improvement in the fitness of single cells ($t_{86} = 2.132$, $P = 0.036$; Fig. 4b and Extended Data Table 1a). Improvement in the fitness of evolved lines can be explained solely by improvement in individual cell performance. The striking response observed under the CE regime can therefore be attributed to a life cycle of alternating phases.

To explore adaptations of the CP regime that contributed to increased lineage performance, life history properties were determined relative to ancestral types, as for the CE regime. No increase was seen in the capacity for WS types to transition to SM. Indeed, a significantly lower proportion of the derived groups produced SM ($\chi^2 = 8.199$, df $= 1$, $P = 0.0042$) and SM types took longer to arise (Extended Data Fig. 8a), hinting at the possibility that cheater suppression might have begun to evolve under this regime (Extended Data Figs 8b–d).

Under the CP regime enhanced line fitness in the derived lineages is explained by changes in traits that improve the competitive ability of individual cells (Extended Data Figs 5c, d and Extended Data Table 2). Enhanced line fitness under the CP regime can be viewed as a by-product of selection at the lower (cell) level. The rate of transition between WS and SM correlates negatively with cell fitness parameters and is not associated with the CP-line fitness. In contrast to the CE regime, in which the WS to SM transition rate increased in a manner interpretable as a consequence of selection at the level of collectives, this trait decreased in the CP regime consistent with selection operating at the cell level. Evolution of this trait in opposing directions can be viewed as resulting from selection at different levels.

Perspective

Multicellular organisms are descendants of once free-living cells[1,3,4]. By virtue of their capacity for differential reproduction, ancestral free-living cells were units of selection[33]. During the transition to multicellularity, collectives of cells emerged that came to participate in Darwinian processes in their own right[2,5,11,19]. The essential ingredient was a means of collective reproduction[5,11]. This most seminal of Darwinian properties emerges afresh at each transition and requires explanation[44]. Here we have shown that cheating cells—those types seemingly most detrimental to the persistence of newly formed cooperative entities—can

function as a germ line within a life cycle that facilitates the reproduction of collectives. Moreover, the two-phase life cycle presents selection with an altogether new kind of biological entity: each state becomes a different attribute of a single organism whose evolution is unified through a developmental programme[45]. When reproduction of collectives is via fragmentation (a single-phase life cycle), the traits that yield success at the higher level are largely those that determine success of single cells. This offers limited opportunity for the emergence of new kinds of biological individuality because properties of higher and lower levels remain aligned[19,38].

Direct observation of early stages in an evolutionary transition requires that issues surrounding levels of selection be considered[2,5,19]. This necessarily leads to territory in which a range of perspectives is possible (see Supplementary Discussion). Our experimental design incorporates an ecology that is explicitly multi-level: both individual cells (that reproduce once every hour), and individual lineages (that reproduce once every 9 days) can be units of selection; however, selection operates on cells and lineages over different timescales. While selection on individual cells favours short-term success, short-term success is unlikely to facilitate persistence of lineages. Indeed, persistence requires more than simply switching between phenotypes: it involves a developmental programme that underpins expression of a collective phase in which a soma-like body is constructed from germ-like cells. Cells of the body must simultaneously play an ecological role (maintaining the body near oxygen via a robust mat phenotype) while producing the seeds of the next generation of bodies (the germ-like cells). Given sufficient variation among lineages, then selection over the longer timescale stands to conquer the short-term interests of individual cells. This appears to have happened in our CE regime with decoupling of fitness between levels supporting the view that selection has begun the process of transitioning to the higher (collective) level—with the lower level beginning to function for the good of the collective.

Online Content Methods, along with any additional Extended Data display items and Source Data, are available in the online version of the paper; references unique to these sections appear only in the online paper.

Received 3 November 2013; accepted 22 September 2014.

1. Bonner, J. T. The origins of multicellularity. *Integr. Biol.* **1,** 27–36 (1998).
2. Okasha, S. *Evolution and the Levels of Selection* (Oxford Univ. Press, 2006).
3. Maynard Smith, J. & Szathmary, E. *The Major Transitions in Evolution* (Oxford Univ. Press, 1995).
4. Buss, L. W. *The Evolution of Individuality* (Princeton Univ. Press, 1987).
5. Godfrey-Smith, P. *Darwinian Populations and Natural Selection* (Oxford Univ. Press, 2009).
6. Nowak, M. A. Five rules for the evolution of cooperation. *Science* **314,** 1560–1563 (2006).
7. Sachs, J. L., Mueller, U. G., Wilcox, T. P. & Bull, J. J. The evolution of cooperation. *Q. Rev. Biol.* **79,** 135–160 (2004).
8. Rainey, P. B. & De Monte, S. Resolving conflicts during the evolutionary transition to multicellular life. *Annu. Rev. Ecol. Evol. Syst.* **45,** 599–620 (2014).
9. Rainey, P. B. & Rainey, K. Evolution of cooperation and conflict in experimental bacterial populations. *Nature* **425,** 72–74 (2003).
10. Pfeiffer, T., Schuster, S. & Bonhoeffer, S. Cooperation and competition in the evolution of ATP-producing pathways. *Science* **292,** 504–507 (2001).
11. Maynard Smith, J. in *Evolutionary Progress* (ed. Nitecki, M. H.) 219–230. (Univ. Chicago Press, 1988).
12. Sober, E. & Wilson, D. S. *Unto Others: The Evolution and Psychology of Unselfish Behaviour* (Harvard Univ. Press, 1998).
13. Velicer, G. J., Kroos, L. & Lenski, R. E. Developmental cheating in the social bacterium *Myxococcus xanthus. Nature* **404,** 598–601 (2000).
14. Strassmann, J. E., Zhu, Y. & Queller, D. C. Altruism and social cheating in the social amoeba *Dictyostelium discoideum. Nature* **408,** 965–967 (2000).
15. Michod, R. E. Cooperation and conflict in the evolution of individuality. 2. Conflict mediation. *Proc. R. Soc. Lond. B* **263,** 813–822 (1996).
16. Nunney, L. Group selection, altruism, and structured-deme models. *Am. Nat.* **126,** 212–230 (1985).
17. Wade, M. J. & Breden, F. The evolution of cheating and selfish behavior. *Behav. Ecol. Sociobiol.* **7,** 167–172 (1980).
18. Santorelli, L. A. *et al.* Facultative cheater mutants reveal the genetic complexity of cooperation in social amoebae. *Nature* **451,** 1107–1110 (2008).
19. Michod, R. E. *Darwinian Dynamics: Evolutionary Transitions in Fitness and Individuality* (Princeton Univ. Press, 1999).
20. Frank, S. A. Mutual policing and repression of competition in the evolution of cooperative groups. *Nature* **377,** 520–522 (1995).
21. Queller, D. C. Relatedness and the fraternal major transitions. *Phil. Trans. R. Soc. Lond. B* **355,** 1647–1655 (2000).
22. Rainey, P. B. Unity from conflict. *Nature* **446,** 616 (2007).
23. McDonald, M. J., Gehrig, S. M., Meintjes, P. L., Zhang, X. X. & Rainey, P. B. Adaptive divergence in experimental populations of *Pseudomonas fluorescens*. IV. Genetic constraints guide evolutionary trajectories in a parallel adaptive radiation. *Genetics* **183,** 1041–1053 (2009).
24. Rainey, P. B. & Travisano, M. Adaptive radiation in a heterogeneous environment. *Nature* **394,** 69–72 (1998).
25. Bantinaki, E. *et al.* Adaptive divergence in experimental populations of *Pseudomonas fluorescens*. III. Mutational origins of wrinkly spreader diversity. *Genetics* **176,** 441–453 (2007).
26. Goymer, P. *et al.* Adaptive divergence in experimental populations of *Pseudomonas fluorescens*. II. Role of the GGDEF regulator WspR in evolution and development of the wrinkly spreader phenotype. *Genetics* **173,** 515–526 (2006).
27. Spiers, A. J., Kahn, S. G., Bohannon, J., Travisano, M. & Rainey, P. B. Adaptive divergence in experimental populations of *Pseudomonas fluorescens*. I. Genetic and phenotypic bases of wrinkly spreader fitness. *Genetics* **161,** 33–46 (2002).
28. Tarnita, C. E., Taubes, C. H. & Nowak, M. A. Evolutionary construction by staying together and coming together. *J. Theor. Biol.* **320,** 10–22 (2013).
29. Trivers, R. L. The evolution of reciprocal altruism. *Q. Rev. Biol.* **46,** 35–57 (1971).
30. Rainey, P. B. & Kerr, B. Cheats as first propagules: a new hypothesis for the evolution of individuality during the transition from single cells to multicellularity. *Bioessays* **32,** 872–880 (2010).
31. Libby, E. & Rainey, P. B. A conceptual framework for the evolutionary origins of multicellularity. *Phys. Biol.* **10,** 035001 (2013).
32. Libby, E. & Rainey, P. B. Eco-evolutionary feedback and the tuning of proto-developmental life cycles. *PLoS ONE* **8,** e82274 (2013).
33. Lewontin, R. C. The units of selection. *Annu. Rev. Ecol. Syst.* **1,** 1–18 (1970).
34. Wolpert, L. & Szathmary, E. Multicellularity: evolution and the egg. *Nature* **420,** 745 (2002).
35. Leigh, E. G. How does selection reconcile individual advantage with the good of the group? *Proc. Natl Acad. Sci. USA* **74,** 4542–4546 (1977).
36. Nunney, L. Lineage selection and the evolution of multistage carcinogenesis. *Proc. R. Soc. Lond. B* **266,** 493–498 (1999).
37. Damuth, J. & Heisler, I. L. Alternative formulations of multi-level selection. *Biol. Philos.* **3,** 407–430 (1988).
38. Michod, R. E. & Roze, D. in *Mathematical and Computational Biology: Computational Morphogenesis, Hierarchical Complexity, and Digital Evolution* (ed. Nehaniv, C. L.) 47–92 (American Mathematical Society, 1999).
39. Okasha, S. Emergence, hierarchy and top-down causation in evolutionary biology. *Interface Focus* **2,** 49–54 (2012).
40. De, N. *et al.* Phosphorylation-independent regulation of the diguanylate cyclase WspR. *PLoS Biol.* **6,** e67 (2008).
41. Levinson, G. & Gutman, G. A. Slipped-strand mispairing: a major mechanism for DNA sequence evolution. *Mol. Biol. Evol.* **4,** 203–221 (1987).
42. Moxon, E. R., Rainey, P. B., Nowak, M. A. & Lenski, R. E. Adaptive evolution of highly mutable loci in pathogenic bacteria. *Curr. Biol.* **4,** 24–33 (1994).
43. Heilbron, K., Toll-Riera, M., Kojadinovic, M. & MacLean, R. C. Fitness is strongly influenced by rare mutations of large effect in a microbial mutation accumulation experiment. *Genetics* **197,** 981–990 (2014).
44. Griesemer, J. The units of evolutionary transition. *Selection* **1,** 67–80 (2001).
45. Wolpert, L. The evolution of development. *Biol. J. Linn. Soc.* **39,** 109–124 (1990).

Supplementary Information is available in the online version of the paper.

Acknowledgements We thank S. Nestmann for assistance with molecular aspects of the work and for guiding construction of the *mutS* deletion mutant. We thank E. Libby and Y. Pichugin for discussion, and S. De Monte and P. G. Smith for comments on drafts of the manuscript. We are indebted to PacBio and particularly J. Korlach and Y. Song for genome sequencing. P.B.R. currently holds an International Blaise Pascal Research Chair funded by the French State and the Ile-de-France, managed by the Fondation de l'Ecole Normale Supérieure. The work was directly supported by the Marsden Fund Council from government funding administered by the Royal Society of New Zealand, and in part by grant RFP-12-20 from the Foundational Questions in Evolutionary Biology Fund, by the National Science Foundation under Cooperative Agreement Number DBI-0939454, and by an NSF CAREER Award Grant (DEB0952825).

Author Contributions All authors contributed to the conception and design of the study. K.H. and C.J.R. performed research, undertook data analysis and prepared figures. All authors wrote the paper.

Author Information All genome data have been deposited into the Sequence Read Archive under accession number SRP047104. P.B.R. will make strains available to qualified recipients. Reprints and permissions information is available at www.nature.com/reprints. The authors declare no competing financial interests. Readers are welcome to comment on the online version of the paper. Correspondence and requests for materials should be addressed to P.B.R. (p.b.rainey@massey.ac.nz).

METHODS

Strains and medium. *Pseudomonas fluorescens* SBW25 (ref. 46) was grown at 28 °C in 25-ml static glass microcosms containing 6 ml of King's Medium B (with loose caps), and on King's Medium B agar plates for 48 h. For competitive assays, strains marked with *lacZ* (ref. 47) allowed types to be distinguished by plating on media containing 60 μg ml^{-1} X-gal.

CE regime. The CE regime (Fig. 1a, left panel) involved a two-phase life cycle (Fig. 1b). The experiment was founded by a single ancestral SBW25 genotype that initiated phase II. After 3 days of static incubation (phase II), 1.5×10^{-7} ml (50 μl of a 3.35×10^{5}-fold dilution) was plated and a single WS colony of the most abundant morphotype was picked from each plate to inoculate a fresh microcosm (Fig. 1b). This marked the start of phase I of the first generation. Following 6 days of static incubation (phase I), microcosms were visually inspected to check for the presence of an intact mat. Lines that had no mat at day six were deemed extinct. Microcosms containing lines with intact mats were vortex mixed and 2.5×10^{-8} ml (200 μl of a 8.0×10^{6}-fold dilution) plated on solid media. After 48 h incubation plates were inspected. To avoid extinction and successfully passage to phase II it was necessary for lines to have produced SM types. All SM colonies were transferred to 200 μl liquid medium and incubated for 24 h under static conditions. The pooled set (from each microcosm) were mixed and 6 μl was used to inoculate phase II microcosms.

CP regime. The CP regime (Fig. 1a, right panel) was identical to the CE regime except that during the life cycle cheats were purged and WS founded both phases of the cycle. Both regimes were conducted in parallel.

Between-lineage selection. Each treatment consisted of 15 replicates of 8 competing microcosms, and replicates from both treatments were spread evenly across 4 experimental blocks. All microcosms in the CE regime were subjected to the selection regime outlined above; however, following assessment of mat integrity at the end of phase I, surviving lineages within each replicate were harvested by vortex-mixing and dilutions spread on agar plates (Fig. 2a). Extinct lineages (due to mat collapse/no mat/no SM colony post phase I, or no WS colony post phase II) were immediately replaced by randomly chosen surviving lines taken from the same replicate. On rare occasions all eight lines of a replicate were eliminated: in these instances one line, chosen at random, from the same experimental block, was used to re-found the replicate. The CP treatment was carried out as above, differing only following phase I when WS colonies were picked instead of SM colonies (Fig. 4a). A smaller volume (6.25×10^{-9} ml (50 μl of a 8.0×10^{6}-fold dilution)) was plated due to the absence of a phenotype-switching requirement for the CP treatment. Both treatment regimes were implemented for ten generations.

Selection of representative WS genotypes. One single WS genotype to represent each replicate from the derived CE and CP 'between-lineage selection regimes' was generated after ten generations as described in Extended Data Fig. 1. The representative WS colonies were grown in shaken microcosms (16 h) and stored at −80 °C for post-selection analyses. This yielded 15 such types each for the ancestral and CP regimes, and 14 types for the CE regime (bacteria from one CE line could not be revived from the freezer stock).

A *lacZ*-marked reference strain (W1-*lacZ*) for fitness comparisons in the CP regime (Extended Data Fig. 1b) was generated the same way from 3-day static microcosms inoculated with a *lacZ*-marked ancestral strain SBW25-*lacZ* (ref. 47).

Fitness assay. Lineage- and cell-level fitness was assessed for all 44 representative ancestral and derived types (Extended Data Fig. 1b). The representative types were not directly competed against each other but against a single, neutrally marked reference strain assayed under the appropriate regime: the ancestral and derived CE types were competed against SBW25-*lacZ*, and the ancestral and derived CP types were competed against W1-*lacZ*. This yielded independent fitness values for each type (that is, potential interactions between ancestral and derived types didn't affect the result), and allowed for estimates and comparison of relative performance for all types.

One lineage generation was performed for each of three replicate fitness assays for all 44 representative types (as shown in Extended Data Fig. 1b for one CE and one CP replicate). For each representative type, eight microcosms were each inoculated with one WS colony in phase I. After mat assessment surviving microcosms were pooled, and 2×10^{-7} ml (200 μl of a 1.0×10^{6}-fold dilution) (CE) or 5×10^{-8} ml (50 μl of a 1×10^{6}-fold dilution) (CP) of this mixture plated. The total number of colonies (in mats) was recorded as a measure of cell fitness. All SM (CE) and WS (CP) colonies, and colonies of the competitor strains SBW25-*lacZ* and W1-*lacZ* were grown overnight and subsequently pooled as described above (CE regime). The derived and ancestral types were mixed with the competitor strains in proportion to their performance during phase I (details displayed in Extended Data Fig. 1b). Six microlitres of this mixture was used to inoculate the eight phase II microcosms. After three days of static incubation (phase II), microcosms were plated. The most abundant WS colony morphotype on each plate determined whether the ancestral/derived representative type or the marked reference type was more successful. The fitness of types representative of each line was calculated for each replicate of eight microcosms as the number of successful offspring of this type as a proportion of the total number of potential offspring (Extended Data Fig. 1b).

Life-history analysis. Static microcosms (36 per representative genotype) were individually inoculated with single colonies of the representative WS types (1,584 microcosms in total). Each day, three replicates were destructively harvested, plated, and the number of SM and WS colony forming units per microcosm was recorded. phase I was extended from 6 to 12 days, phase II from 3 to 6 days. At day six, propagules were collected for phase II, and microcosms inoculated (18 per type). Each day, three replicate microcosms per representative type were destructively harvested and number of SM and WS colony forming units recorded.

SM growth assay. Three biological replicate SM colonies were derived from each of the representative ancestral and derived CE and CP WS types. Four day static microcosms seeded from a single WS colony were destructively harvested and plated (5×10^{-8} ml). SM colonies were chosen, grown in shaken microcosms (16 h), and stored at −80 °C. This procedure was repeated until three biological SM replicate colonies were obtained. For the types where three biological replicate SM colonies couldn't be derived, additional experimental replicates of SM growth rate were assessed. In a small number of instances no SM types were obtained.

SM growth kinetics were determined in 96-well microtitre plates shaken at 28 °C, and absorbance (OD_{600}) measured in a microplate reader (BioTek). Each well was inoculated with approximately 10^{4} SM cells in 180 μl King's medium B and absorbance measured every 10 min for 24 h. The growth of each biological replicate was determined in three different well locations on independent 96-well plates and on separate days. The maximum growth rate (V_{max}) was calculated from the maximum slope of the absorbance over time. The mean V_{max} for each representative type was calculated from all biological and experimental SM replicates.

Statistical analysis. For detecting differences in line level fitness between the ancestral and derived regimes, a generalized linear model (error structure: binomial; link function: logit) with the explanatory variables regime, and representative type (nested within regime) was calculated. Contrasts revealed differences in lineage level fitness between regimes.

Analysis of variance (ANOVA) was used to test for differences in total number of cells, number of WS per μl, number of SM per μl (if present), and SM growth rate between the different regimes. Explanatory variables were regime, and representative type (nested within regime). Post hoc contrasts revealed differences between the ancestral and their respective derived regime.

Generalized linear models (error structure: binomial; link function: logit) were used to test for the difference between regimes in life-history parameters during the course of the experiment. The response variable was 'proportion of microcosms with the new type'. Explanatory variables were regime, representative type (nested within regime), and time. Analysis of variance was performed with the same explanatory variables but for 'new cell type per μl', 'total cells per μl', and 'proportion of the new cell type within a microcosm'. All three variables were Box–Cox transformed. Contrasts revealed differences between the regimes on the individual days.

Relationships between all parameters were tested using the mean per representative type accounting for regime. Pearson and Spearman rank correlations, and regressions (line level fitness: generalized linear models with the normal error structure, and the identity link function; cell-level fitness and number of SM per μl (if present): general linear models) were performed. SM growth rate, number of SM per μl (if present), and SM/WS occurrence were Box–Cox transformed.

Colony counts from contaminated plates were excluded from analyses. Sample size was chosen to maximise statistical power and ensure sufficient replication. Assumptions of the tests, that is, normality and equal distribution of variances, were visually evaluated. Non-significant interactions were removed from the models. All tests were two-tailed. Effects were considered significant at the level of $P < 0.05$. All statistical analyses were performed with JMP 9. Graphs were produced with GraphPad Prism 5.0, JColorgrid (http://jcolorgrid.sourceforge.net), Adobe Illustrator CC 17.0.0 and Inkscape 0.48.2.

Genetic manipulation. Standard genetic techniques were used to revert *mutS* (A1489C) to wild type. This involved PCR amplification of the wild-type sequence from SBW25 and its integration into the genome of WS_{22} by homologous recombination facilitated by a two-step allelic replacement strategy using pUIC-3 (ref. 27). Characterization of G-tract expansion and contraction in *wspR* was performed by PCR and Sanger sequencing.

Genome sequencing. Genomic DNA was extracted from overnight cultures (each founded by a single colony) using Wizard Genomic DNA Purification Kit (Promega), and sent to the Australian Genome Research Facility and Pacific Biosciences, for Illumina and SMRT sequencing, respectively. Libraries for SMRT sequencing were prepared on a Sciclone NGS automated liquid handling workstation (Perkin Elmer, Waltham MA) using a 10-kb automated library preparation protocol (Pacific Biosciences, Menlo Park, CA) which includes an initial Solid Phase Reversible Immobilization (SPRI) clean-up step, followed by the standard 10-kb library preparation protocol. Libraries were annealed using 20× excess primer using the standard annealing

protocol (Pacific Biosciences). Sequencing was performed on the PacBio RSII using P4-C2 sequencing chemistry, magnetic bead loading, and 3-h movie acquisitions. Sequence reads were mapped against the *P. fluorescens* SBW25 GenBank reference and variants were called using SMRTPortal version 2.3. Additional analyses were performed with Geneious 7.1.4.

46. Silby, M. W. *et al.* Genomic and genetic analyses of diversity and plant interactions of *Pseudomonas fluorescens. Genome Biol.* **10,** R51 (2009).
47. Zhang, X. X. & Rainey, P. B. Construction and validation of a neutrally-marked strain of *Pseudomonas fluorescens* SBW25. *J. Microbiol. Methods* **71,** 78–81 (2007).

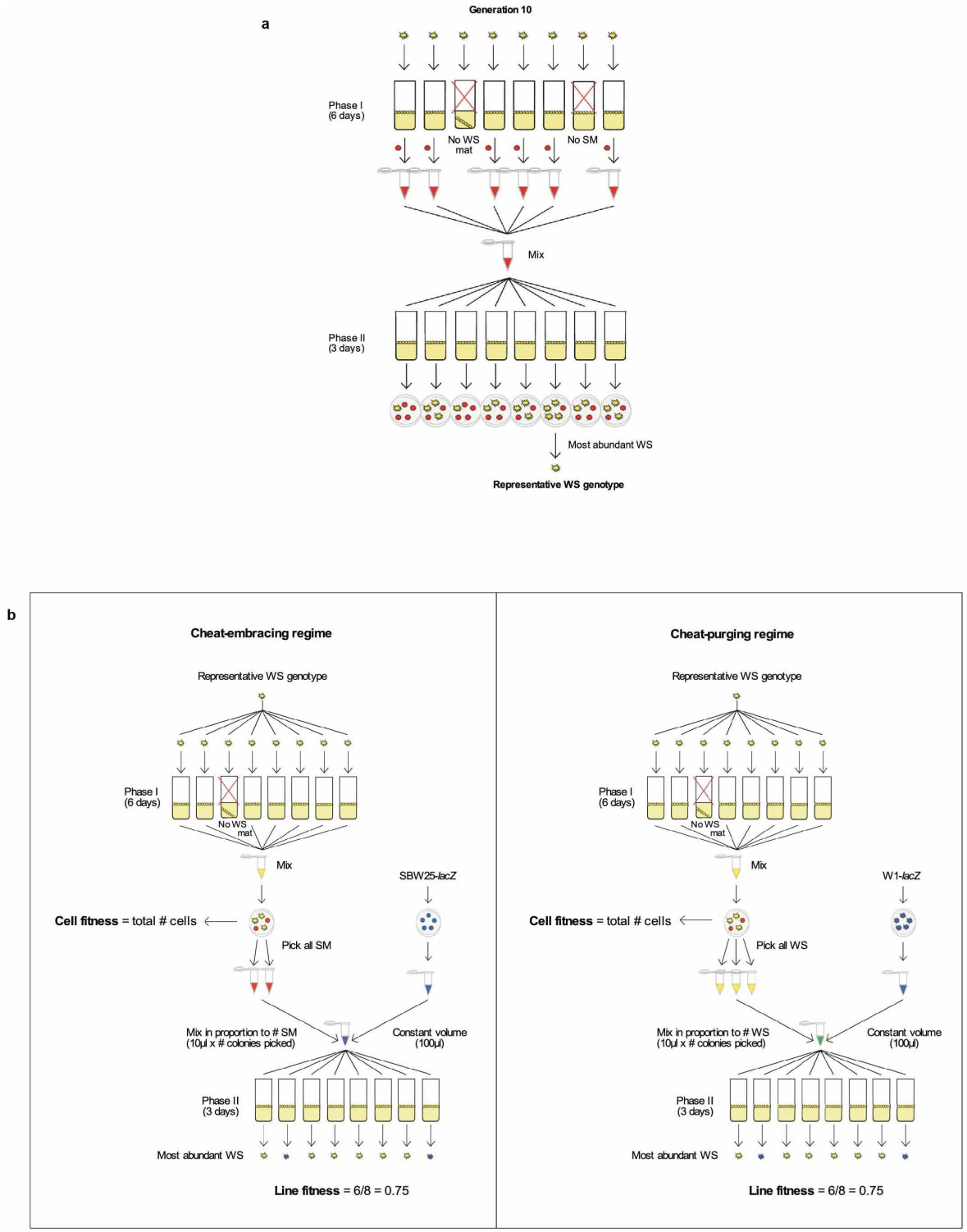

Extended Data Figure 1 | Representative WS genotypes and fitness assays. **a**, To analyse the response of derived lines to selection, a single representative WS genotype was obtained from each replicate population (set of eight microcosms) from both ancestral and derived lines. To obtain the representative set of derived types under the CE regime, SM colonies were collected from the end of phase I at generation 10 and pooled. The pooled sample was used to found phase II, at the end of which a single WS-type representative of each replicate was selected as described for the baseline (see below). This yielded 14 such types, one representing each replicate. To obtain the set of baseline types representing the ancestral state, SBW25 was used to found phase II. At the end of the 3-day period lines were harvested and plated. The single most abundant WS type from the most densely populated plate was selected as representative of that replicate. A third set of representative WS genotypes was obtained from lines evolved under the CP regime. This was as for the CE regime, but instead of pooling SM at the end of phase I, WS were collected and pooled. A single dominant WS type was chosen from each replicate. **b**, Cell- and line-fitness assays. Lines founded by representative WS genotypes (from ancestral and derived lineages) were competed against a marked (blue colonies) reference strain (SM and WS, for the CE and CP regimes, respectively). Use of the marked reference strain allowed the competitive performance of all ancestral and derived types to be assessed against a single common genotype. Cell fitness is the total number of cells in the mat after phase I, whereas line fitness is the proportion of evolved 'offspring' mats relative to a marked reference strain. In total 2,472 microcosms were assayed (three replicate assays per line).

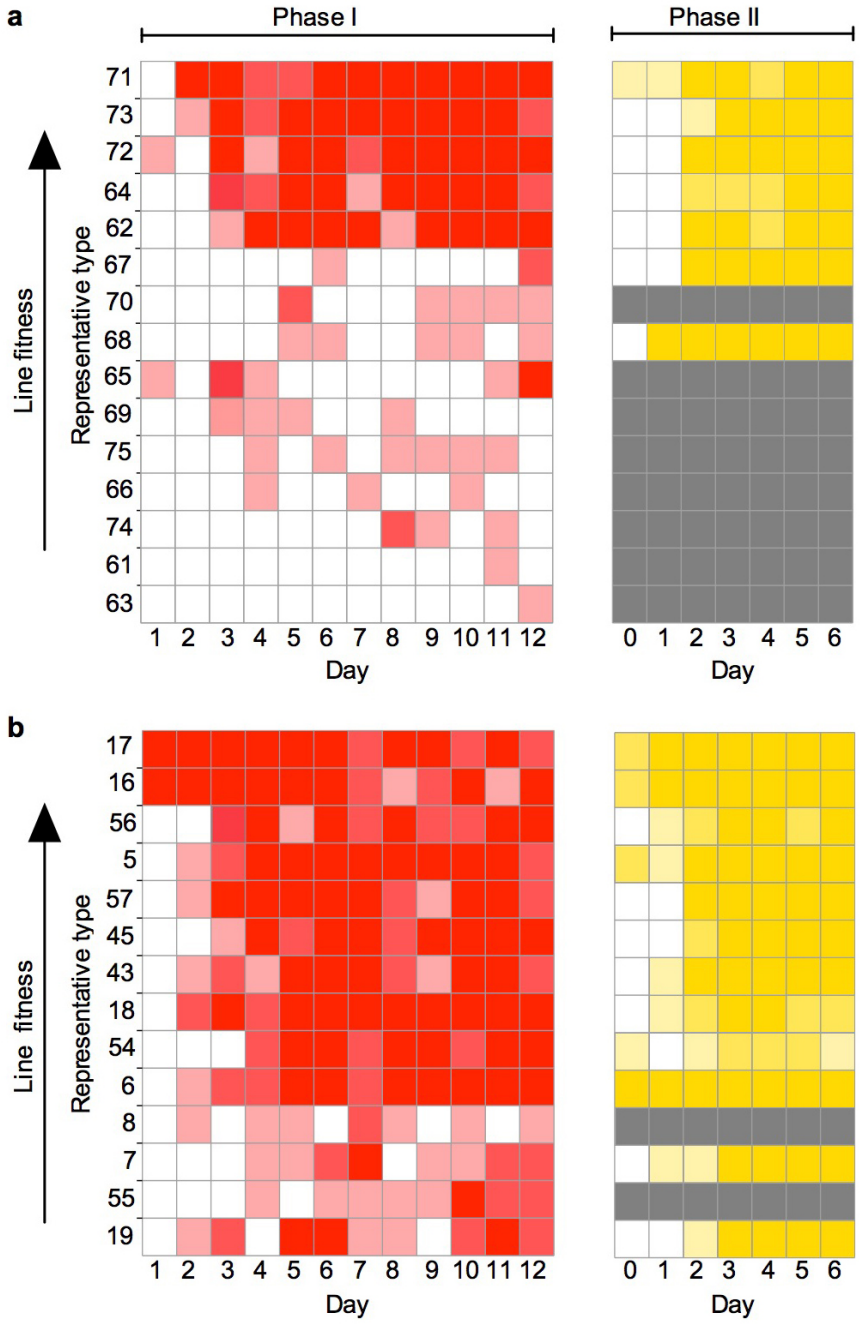

Extended Data Figure 2 | Line fitness and life cycle perpetuation. **a**, **b**, Fitness of ancestral (**a**) and derived (**b**) lines and relationship with capacity to perpetuate the two-phase life cycle. Data are a breakdown of data in Fig. 3a. Colour intensity represents the proportion of three replicate microcosms harbouring the new type (white, absence of new type; dark red (yellow), presence of SM (WS) in all microcosms). Lines are ordered according to their fitness as assayed under the CE regime. Grey cells indicate loss of lines due to extinction.

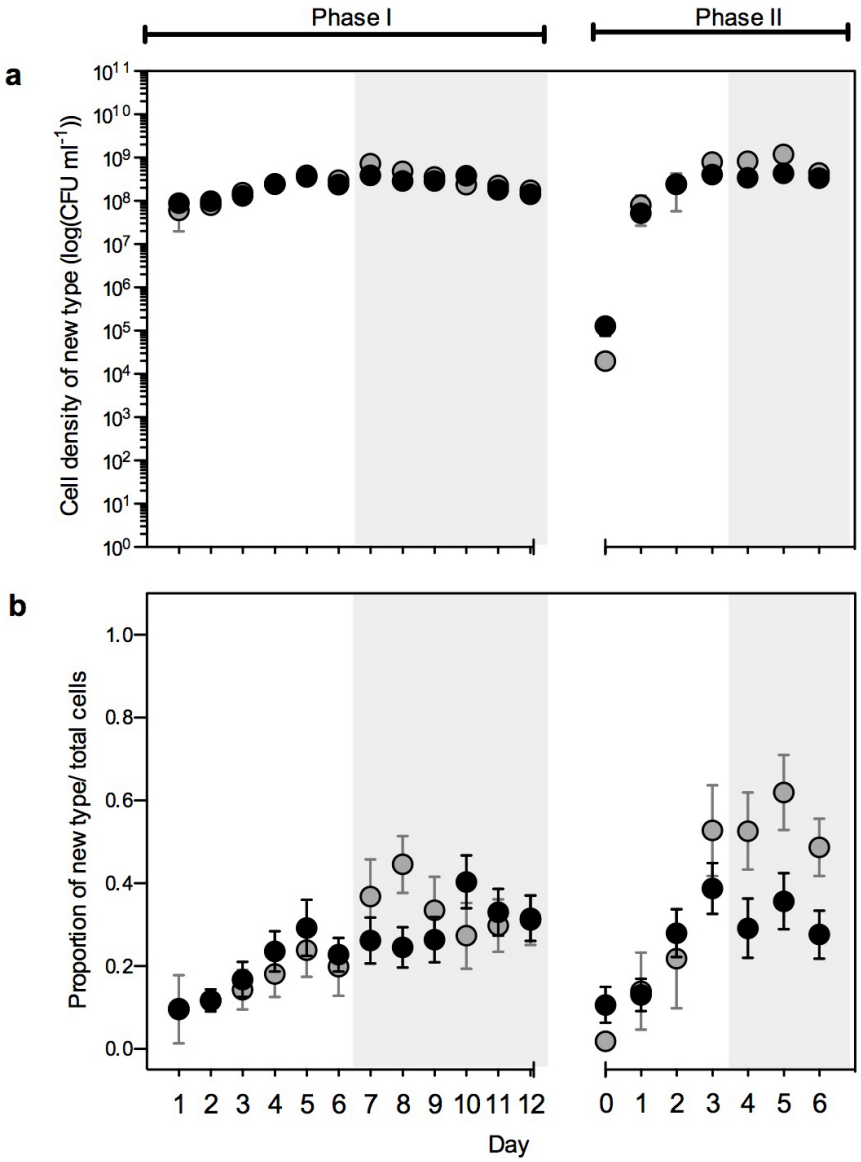

Extended Data Figure 3 | Life history traits under the CE regime. **a**, Cell density of the new type. **b**, Proportion of the new cell type divided by the total number of cells. Each circle represents the mean of 42–45 lines (that is, three replicates for each of the 15 ancestral and 14 derived lines). Lines that failed to produce the required type were excluded. Black, derived; grey, ancestral. Error bars are s.e.m., based on $n \leq 15$. $^{*}P < 0.05$, using analysis of variance (ANOVA) and post hoc contrasts.

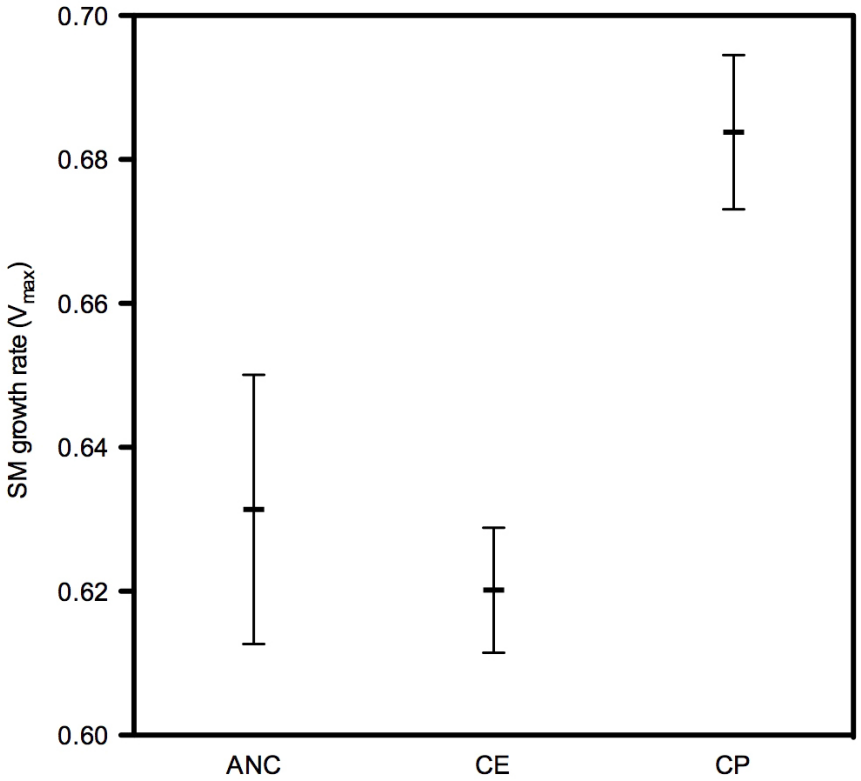

Extended Data Figure 4 | Growth rate of SM. Growth rate of the ancestral (ANC) and derived SM types from the CE and CP regimes obtained from the representative genotypes (biological and technical replicates; see Methods). (ANC, $n = 81$; CE, $n = 95$; CP $n = 81$). Error bars are s.e.m., based on $n \leq 15$.

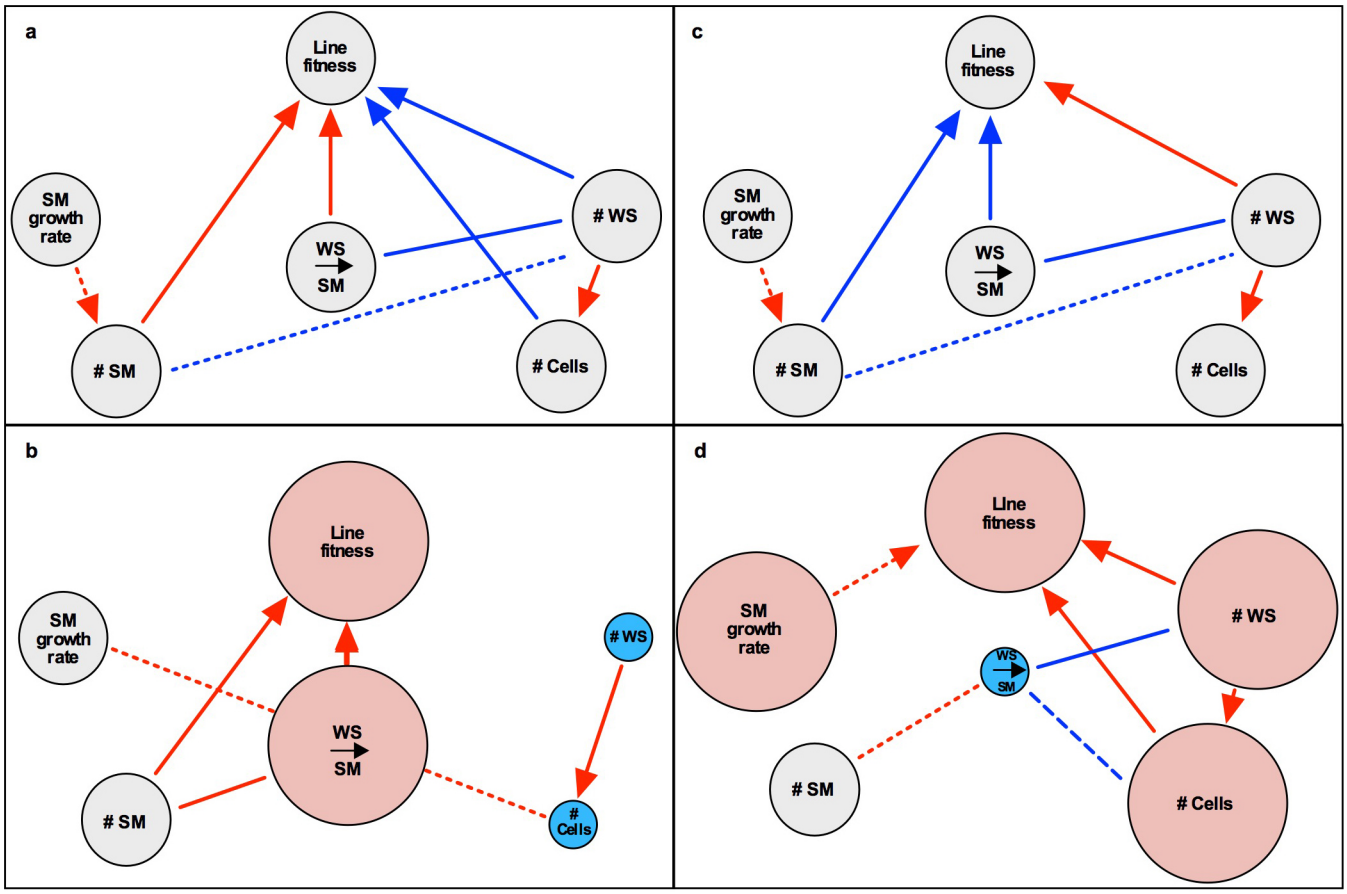

Extended Data Figure 5 | Relationship between fitness and associated traits. **a**–**d**, Summary of parameters describing line and cellular properties and the relationship among these parameters in ancestral (**a**) and derived (**b**) CE and ancestral (**c**) and derived (**d**) CP populations. Traits in the evolved populations (**b**, **d**) are depicted relative to their respective ancestral states (**a**, **c**): significant increase (large red circle), significant decrease (small blue circle), and no significant change (grey circle) using a generalized linear model (error structure: binomial; link function: logit) for line fitness and WS→SM with post hoc contrasts; and analysis of variance (ANOVA) for number of cells, number of WS, number of SM, and SM growth rate with post hoc contrasts. WS→SM, proportion of lines producing SM during phase I. Arrows indicate significant regressions and lines indicate significant correlations between traits, dashed lines indicate trends ($0.05 < P < 0.09$). The colour represents the direction of the relationship: red, positive; blue, negative. The significance level is $P < 0.05$ using Pearson and Spearman rank correlations, and regressions (line level fitness: generalized linear models; cell-level fitness and number of SM per µl (if present): general linear models). Individual cell properties displayed in **a** and **c** are identical for the ancestral state in both CE and CP regimes, but measures of line fitness are regime-specific, and transform the associations between parameters. Parameters that relate positively to line fitness in the CE regime negatively affect line fitness in the CP regime, and vice versa (**a** versus **c**). For example, in the CE regime, the number of SM cells and the rate at which WS cells give rise to SM cells positively regresses on line fitness (red arrows, **a**), whereas only the number of WS cells shows a positive regression with line fitness in the CP regime (red arrows, **c**). The relationships between parameters in the ancestral populations predict their evolutionary trajectory in each regime. After 10 generations of line selection the relationships between cell- and line-level parameters significantly altered in both CE and CP regimes (**b** and **d**). Line fitness improved in both regimes, thereby imposing selection on parameters that were linked to line fitness in their respective baselines. In the CE regime enhanced line fitness is explained by a significant increase in the capacity to transition from WS to SM and is not explained by enhanced performance of single cells: the fitness of single cells either remained unaltered or declined. Increased line fitness can be seen as a product of selection at the higher (group) level. In marked contrast is the CP regime where improved line fitness is readily explained by changes in traits that improve the competitive ability of individual cells. Enhanced line fitness in the CP regime can be interpreted as a by-product of selection at the lower (cell) level.

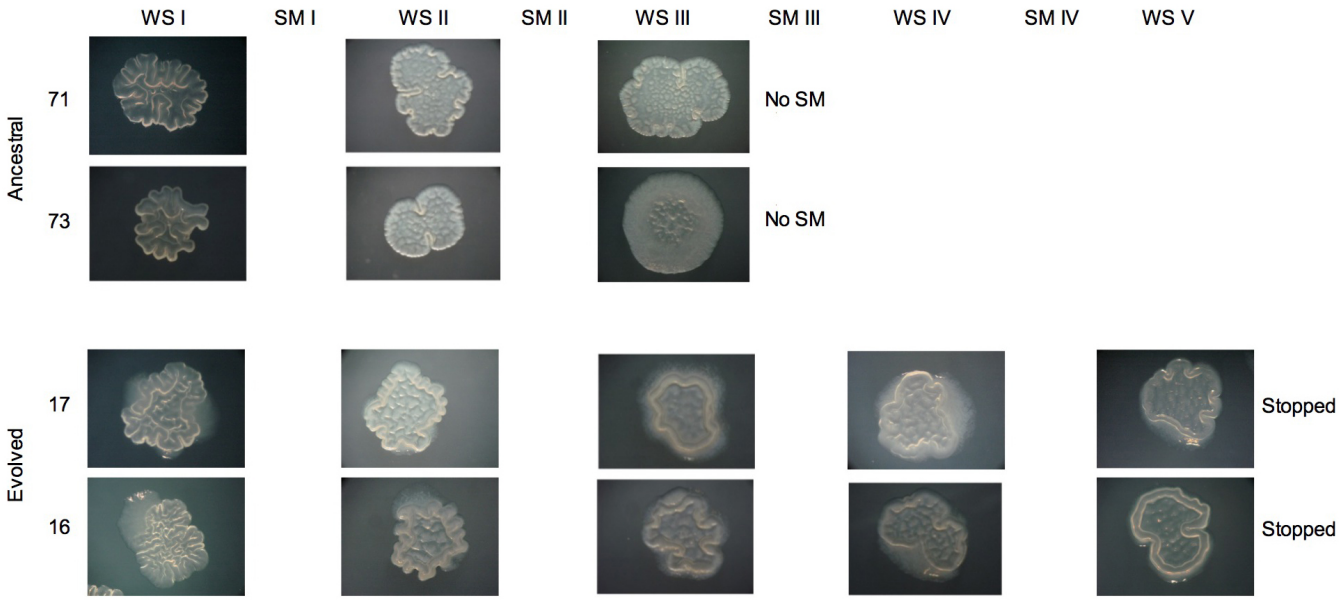

Extended Data Figure 6 | Cycling through phases. Ancestral and derived lines differ in their capacity to transition between phases of the life cycle. Three replicate populations of the two ancestral and derived lineages with the highest fitness: 71, 73 and 16, 17, respectively, were founded by the representative WS type and plated to check for SM types. Whereas ancestral WS took 48 h to generate detectable levels of SM, the two derived WS populations contained a mixture of WS and SM colonies, such that even at the time of initial inoculation, both types were present. SM colonies were then used to found populations that were plated to check for WS types. Ancestral lineages 71 and 73 completed two cycles before extinction through failure to produce SM, whereas derived lines 16 and 17 completed five cycles before termination of the experiment. Colonies were photographed after 48 h of growth. Notable in the evolved lines is the visible presence of zones of SM cells surrounding the central WS colony.

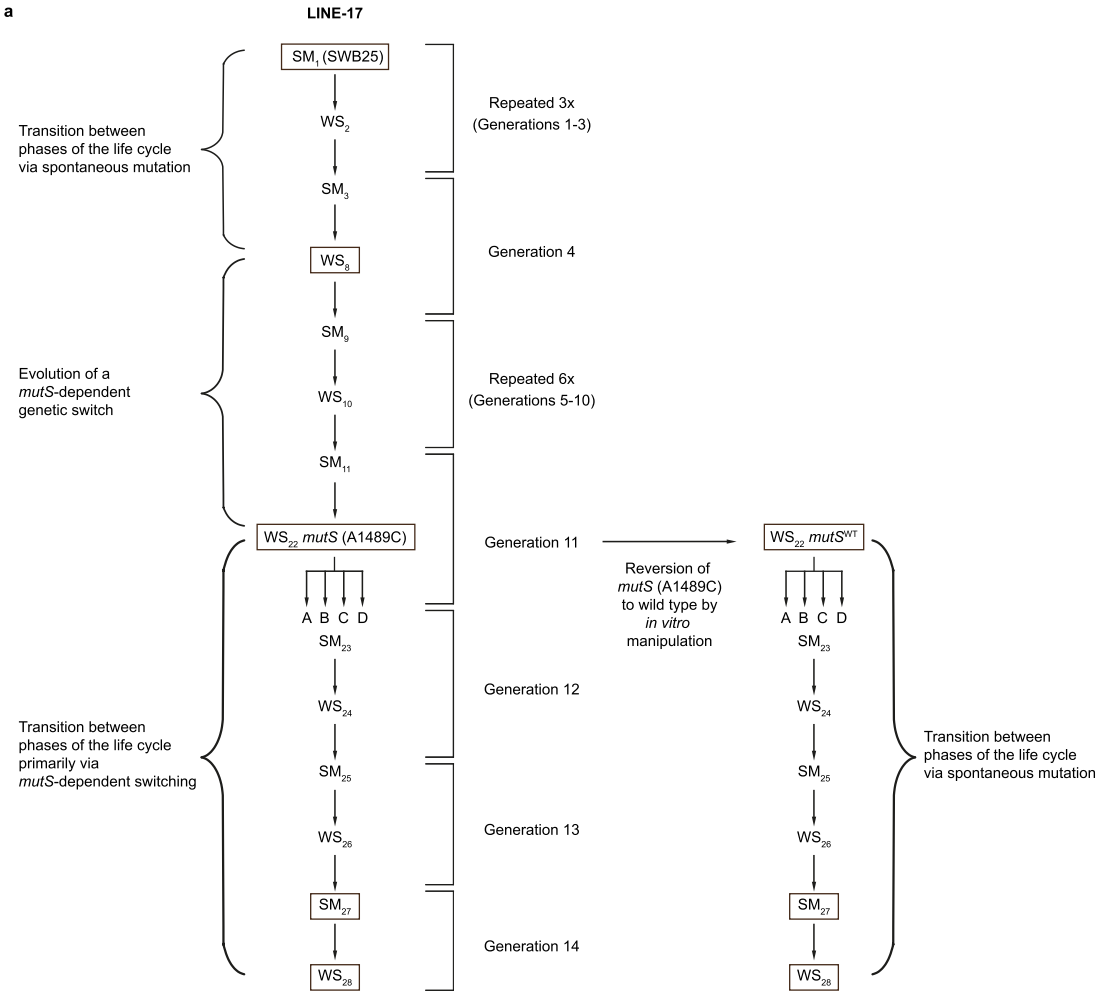

Extended Data Figure 7 | Mechanism of life cycle transition. **a**, Outline of the evolutionary history of line 17 from its founding by ancestral SM_1 SBW25 through ten generations of the life cycle, by which time a *mutS* mutation had arisen. At the eleventh generation, the *mutS* (A1489C) mutation in WS_{22} was reverted to wild type ($mutS^{WT}$) by *in vitro* manipulation. The two WS_{22} lineages (with and without the *mutS* mutation) were taken through three additional 'expedited' life-cycle generations, although with a cycling period of 24 h for *mutS* (A1489C) and 48 h for $mutS^{WT}$. Genome sequences were acquired from five different time points (SM_1, WS_8, WS_{22}, SM_{27} and WS_{28}, indicated by surrounding boxes). For details of mutations see Supplementary Table 1. **b**, The *mutS*-dependent genetic switch. Four independent cultures of the generation-11 WS (WS_{22}), with and without the *mutS* (A1489C) mutation, were passaged through an additional three 'expedited' generations of the life cycle (WS_{22}–WS_{28}). The nucleotide sequence of *wspR* was determined at each stage. Depicted is the tract of guanine residues beginning at nucleotide 742: WspR is active (and the phenotype is WS) when the tract length is seven residues, but inactive (and the phenotype is SM) when the tract length is eight. Red arrows show slippage events resulting in the gain or loss of a single guanine residue. Transitioning between phases is more reliable (fewer extinction events) and more likely to occur via the tract of guanine residues in the presence of *mutS* (A1489C). Lines of *mutS* (A1489C) were passaged on a 24-h cycle; $mutS^{WT}$ lines were passaged on a 48-h cycle (on a 24-h cycle $mutS^{WT}$ lines were extinct before the first generation completed—ancestral lines are incapable of transitioning on a 48-h cycle). Extinction events occurred whenever the extant phase failed to produce the next stage in the life cycle; death of a line allowed birth of an extant lineage (diagonal arrows).

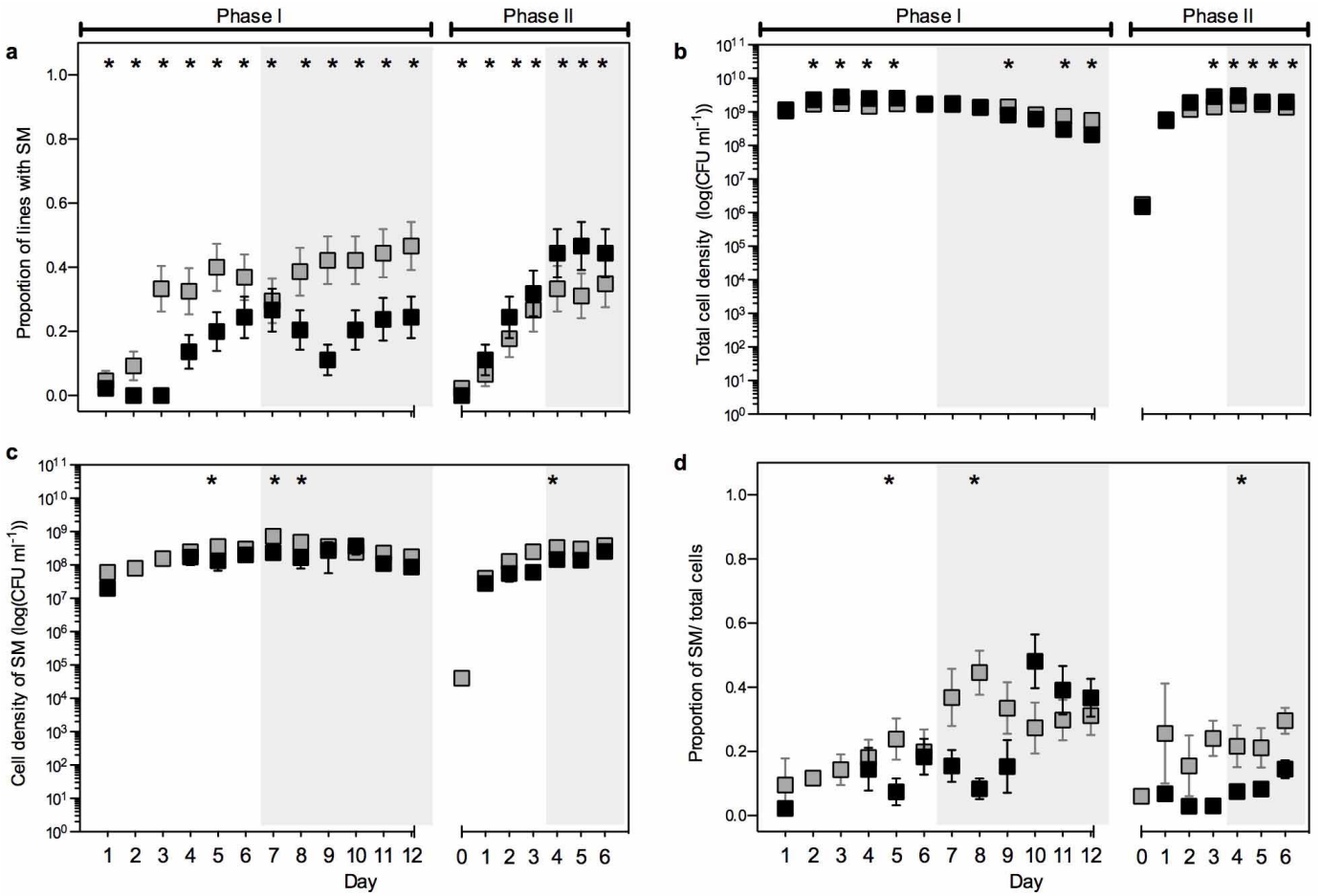

Extended Data Figure 8 | Life history traits under the CP regime. **a**, Proportion of lines producing SM. **b**, Total cell density. **c**, Cell density of the new type. **d**, Proportion of SM cell types divided by the total number of cells. Each square represents the mean of 45 lines (that is, 3 replicates for each of the 15 lines); however, for **c** and **d** lines that failed to produce SM were excluded. Black, derived; grey, ancestral. Error bars are s.e.m., based on $n \leq 15$. *$P < 0.05$, using a generalized linear model (error structure: binomial; link function: logit) and post hoc contrasts for **a**; and using analysis of variance (ANOVA) and post hoc contrasts for **b**–**d**.

Extended Data Table 1 | Differences in life history parameters

a

Parameters	N	df	F/χ^2	P	R^2
Line fitness			χ^2		
Full model	1392	59	1160.211	**<0.0001**	
Regime		3	61.429	**<0.0001**	
Rep. type (Regime)		56	1090.351	**<0.0001**	
Cell fitness			F		
Full model	126	43	4.404	**<0.0001**	0.698
Regime		2	13.524	**<0.0001**	
Rep. type (Regime)		41	3.916	**<0.0001**	
#WS			F		
Full model	126	43	5.508	**<0.0001**	0.743
Regime		2	28.282	**<0.0001**	
Rep. type (Regime)		41	4.339	**<0.0001**	
#SM X	80		F		
Full model		31	5.148	**<0.0001**	0.769
Regime		2	2.358	=0.1055	
Rep. type (Regime)		29	5.190	**<0.0001**	
SM growth rate			F		
Full model	104	36	6.450	**<0.0001**	0.777
Regime		2	32.806	**<0.0001**	
Rep. type (Regime)		34	5.101	**<0.0001**	
WS → SM			χ^2		
Full model	1557	43	565.727	**<0.0001**	
Regime		2	289.108	**<0.0001**	
Rep. type (Regime)		41	467.060	**<0.0001**	

b

Parameters	N	df	F/χ^2	P	R^2
Proportion of lines with new type			χ^2		
Full model	1357	64	690.216	**<0.0001**	
Regime		1	5.442	**=0.0197**	
Rep. type (Regime)		27	457.619	**<0.0001**	
Time		18	385.403	**<0.0001**	
Regime x Time		18	62.994	**<0.0001**	
Total # cells/µl X			F		
Full model	1355	46	21.697	**<0.0001**	0.433
Regime		1	51.521	**<0.0001**	
Rep. type (Regime)		27	8.144	**<0.0001**	
Time		18	39.887	**<0.0001**	
Regime x Time				n.s.	
# new type/µl X			F		
Full model	740	46	8.823	**<0.0001**	0.369
Regime		1	0.589	=0.4431	
Rep. type (Regime)		27	5.620	**<0.0001**	
Time		18	13.615	**<0.0001**	
Regime x Time				n.s.	
Proportion new cell type X			F		
Full model	740	46	6.447	**<0.0001**	0.300
Regime		1	1.701	=0.1926	
Rep. type (Regime)		27	6.648	**<0.0001**	
Time		18	6.229	**<0.0001**	
Regime x Time				n.s.	

a, Differences in line fitness, cell fitness and life-history traits between ANC, CE and CP regimes. Results from generalized and general linear models are shown. Values for ancestral lines are the same for all parameters measured during phase I, whereas line fitness differs between ancestral CE and CP regimes. Rep. type, representative WS genotype; #WS, number of WS at day 6 within a mat, #SM X, number of SM at day 6 within a mat (SM = 0 were excluded); X, Box–Cox transformation; WS→SM, proportion of lines producing SM during phase I. **b**, Differences in life history traits between ancestral and evolved CE regimes over time. Results from generalized and general linear models are shown (all three parameters were Box–Cox transformed). Bold denotes significance at the level of $P < 0.05$.

Extended Data Table 2 | Relationship between fitness and life history parameters

a

	SM growth X	#SM/µl X	#WS	WS➔SM X	Line fitness	Cell fitness
SM growth X	-	R^2=0.449, F=4.893, P=0.0690, N=8	r=-0.372, P=0.2335, N=12	r=0.222, P=0.4882, N=12	χ^2=0.711, df=1, P=0.3992, N=12	r=-0.218, P=0.4964, N=12
#SM/µl X	R^2=0.007, F=0.087, P=0.773, N=14	-	r_S=-0.667, P=0.0710, N=8	r_S=0.619, P=0.1017, N=8	**χ^2=26.801, df=1, P<0.0001, N=8**	R^2=0.380 $F_{1,8}$=3.671, P=0.1038
#WS	r=0.381, P=0.1796, N=14	r_S =0.007 P=0.9822, N=14	-	**r=-0.689, P=0.0045, N=15**	**χ^2=11.150, df=1, P=0.0008, N=15**	**R^2=0.339, $F_{1,15}$=6.673, P=0.0227**
WS➔SM X	r=0.063, P=0.8297, N=14	**r_S=0.587, P=0.0274, N=14**	r=0.114, P=0.6987, N=14	-	**χ^2=22.801, df=1, P<0.0001, N=15**	r=-0.378, P=0.1645, N=15
Line fitness	χ^2=0.061, df=1, P=0.8046, N=14	**χ^2=9.305, df=1, P=0.0023, N=14**	χ^2=1.008, df=1, P=0.3154, N=14	**χ^2=12.324, df=1, P=0.0004, N=14**	-	**χ^2=4.246, df=1, P=0.0393, N=15**
Cell fitness	r=0.486, P=0.0783, N=14	R^2=0.009, $F_{1,14}$=0.113, P=0.7428	**R^2=0.890, $F_{1,14}$=97.359, P<0.0001**	r=0.326, P=0.2558, N=14	χ^2=2.041, df=1, P=0.1531, N=14	-

b

	SM growth X	#SM/µl X	#WS	WS➔SM X	Line fitness	Cell fitness
SM growth X	-	R^2=0.449, F=4.893, P=0.0690, N=8	r=-0.372, P=0.2335, N=12	r=0.222, P=0.4882, N=12	χ^2=0.705, df=1, P=0.4010, N=12	r=-0.218, P=0.4964, N=12
#SM/µl X	R^2=0.011, F=0.0656, P=0.8064, N=8	-	r_S=-0.667, P=0.0710, N=8	r_S=0.619, P=0.1017, N=8	**χ^2=17.568, df=1, P<0.0001, N=8**	R^2=0.380 $F_{1,8}$=3.671, P=0.1038
#WS	r=0.215, P=0.5265, N=11	r_S=0.222, P=0.5372, N=10	-	**r=-0.689, P=0.0045, N=15**	**χ^2=6.153, df=1, P=0.0131, N=15**	**R^2=0.339, $F_{1,15}$=6.673, P=0.0227**
WS➔SM X	r=0.221, P=0.4129, N=11	r_S=0.616, P=0.0580, N=10	**r=-0.669, P=0.0064, N=15**	-	**χ^2=8.710, df=1, P=0.0032, N=15**	r=-0.378, P=0.1645, N=15
Line fitness	**χ^2=5.567, df=1, P=0.0183, N=11**	χ^2=0.312, df=1, P=0.5762, N=10	**χ^2=7.552, df=1, P=0.0060, N=15**	χ^2=2.129, df=1, P=0.1445, N=15	-	χ^2=0.746, df=1, P=0.3878, N=15
Cell fitness	r=0.290, P=0.3874, N=11	R^2=0.074, $F_{1,10}$=0.640, P=0.4470	**R^2=0.887, $F_{1,15}$=101.583, P<0.0001**	r=-0.473, P=0.0750, N=15	**χ^2=5.339, df=1, P=0.0208, N=15**	-

a, CE regime, and **b**, CP regime. X denotes parameters that were Box–Cox transformed to meet requirements of normality and equal variance. WS→SM, proportion of lines producing SM during phase I. Above the diagonal are tests for the ancestral regimes (grey), below for the evolved regimes (black). Bold denotes significance at the level of $P < 0.05$.